Calorimetric Study of Glassy State. IX. Thermodynamic Properties of Stannous Chloride Dihydrate and Dideuterate Crystals*

Takasuke MATSUO, Masaharu OGUNI, Hiroshi SUGA, and Syûzô SEKI
Department of Chemistry, Faculty of Science, Osaka University, Toyonaka, Osaka 560

Appendix: High Temperature Entropy Calculation

John F. NAGLE
Department of Physics, Carnegie-Mellon University, Pittsburgh, Penn. 15213 USA

(Received September 27, 1973)

The heat capacity of $SnCl_2 \cdot 2H_2O$ and $SnCl_2 \cdot 2D_2O$ crystals, substances with layer structure, was measured from 13 to 300 K. Anomalies due to ordering of the hydrogen (deuterium) position were observed at $T_c(H_2O) = 217.94$ K and at $T_c(D_2O) = 234.47 \pm 0.05$ K. The total entropy change of the transition was estimated to be 4.6 J K^{-1} mol^{-1} for both compounds. An exact calculation of the high temperature entropy based on the two-dimensional lattice model gave 3.13 J K^{-1} mol^{-1}. The critical indices $\alpha_\pm$ of the divergent heat capacity anomalies are as follows: $\alpha_+(H_2O) = 0.53$, $\alpha_-(H_2O) = 0.48$, $\alpha_+(D_2O) = 0.57$, $\alpha_-(D_2O) = 0.54$. Another heat capacity anomaly was found at 140—160 K where the heat capacity values depended on the thermal history of the specimen. The enthalpy relaxation observed at the temperature region was analysed by use of the first-order rate equation, giving the activation enthalpies $\Delta H_a(H_2O) = 49.9$ kJ mol^{-1} and $\Delta H_a(D_2O) = 49.8$ kJ mol^{-1}. The concept of long-range-ordered glassy state was introduced for description of the non-equilibrium state of the present substances below 140 K. A general consideration of the relation between molecular relaxation and phase change in terms of the Deborah number is presented.

Stannous chloride dihydrate has a layer structure in which double layers of the stannous chloride molecules are sandwiched between the hydrogen-bonded networks of the water molecules.[1,2] A phase transition was found in this substance and its deuterate analogue by use of dielectric, nuclear magnetic resonance and electric conductivity measurements,[3] and was attributed to the order-disorder change of the hydrogen positions in the network. Since thermodynamic properties are of special interest in connection with the two-dimensional nature of the crystal structure, we measured the heat capacity of the hydrate and deuterate from 13 to 300 K. Both compounds exhibited sharp heat capacity peak at the transition point. In addition, an unexpected thermal relaxation phenomenon was observed at a lower temperature and could be interpreted quantitatively as caused by a slow ordering process of the hydrogen position. The phenomenon is interesting in connection with the recently proposed concept of the glassy crystalline state.[4]

Experimental

Sample Preparation. Commercially available stannous chloride dihydrate of the highest purity was molten in an air-tight flask (melting point: 40 °C), and cooled slowly in a temperature-controlled water bath. When about half of the material was crystallized, the remaining melt was discarded. The crystal was kept in a closed vessel before use. The water content of the crystal was determined from the weight loss accompanying the dehydration to the anhydrous salt. It was found to be 15.97% in an excellent agreement with the stoichiometric value, 15.96%. Spectrometric analysis of the specimen taken from the calorimeter cell after completion of the measurement showed that impurity ions in the crystal were copper, iron, nickel and calcium, each less than 10 ppm.

Before the above method of fractional melting was found to be successful, recrystallization from the saturated aqueous solution was attempted. The water content of the crystal obtained by this method was consistently higher than the ideal value by 0.2 to 0.3%. Heat capacity of the crystal containing the excess water was also measured from 13 to 300 K, though the main body of the experimental data refers to the crystal obtained by the improved method. Qualitative behaviors of the differently prepared crystals were similar to each other as will be described below.

The deuterate was prepared from the purified hydrate by the similar method as follows. The hydrate was first dehydrated to the stoichiometric anhydrous salt, to which an appropriate quantity of 99.75% heavy water and a small amount of deuterochloric acid were added. The mixture was heated to 45 °C, and when a clear solution was obtained, it was cooled slowly. The crystallization began at about 41 °C. The procedure taken thereafter was similar to that for the hydrate.

Calorimetric Apparatus. The calorimetric system used was the same one described elsewhere,[5] with minor modifications. The hand-set type of the potentiometer formerly used for the electric energy measurement was replaced with a digital voltmeter (Hewlett Packard model 3462 A) and the clock, with a digital time interval counter (Takeda Riken Model TR-5766 U/6). The cryostat, temperature measureing apparatus and the adiabatic control circuit remained unaltered. The overall accuracy of the measurement is believed to be about 1% at 20 K and better than 0.3% above 50 K.

Sample Handling. In order to avoid efflorescence and deliquescence of the specimen, the crystal was handled in a glove box in which the humidity was adjusted to the dissociation pressure of the crystal by placing in the box a quantity of the partially dehydrated crystal. Similar precaution was taken for the deuterate by using the crude deuterate material. The sample crystals were crushed to 2—3 mm in the linear dimension and loaded in the calorimeter cell. The loaded cell, with the gas-filling tube open, was cooled to liquid nitrogen temperature in a glass vessel. The glass vessel was evacuated,

* A brief account of the present paper was published in *Proc. Japan Acad.*, **48**, 237 (1972).

flushed twice, and filled with one atm of helium gas. After being allowed to warm up to the room temperature, the cell was taken out of the glass vessel and the filling tube was sealed promptly with low melting solder. The sample weight was 97.507 g and 92.949 g for the hydrate and the deuterate, respectively.

Calorimetric Procedure. As was stated above the heat capacity was measured first on a sample containing excess water. The calorimeter was first cooled to the liquid nitrogen temperature, at which the first series of measurement was commenced. At temperature around 150 K, a marked upward temperature drift was observed. At about 162 K, it changed to downward drift, indicating a slow equilibration in the calorimeter. An appreciable cooling was observed for more than 45 min after turning off the calorimeter heater, compared to the typical equilibration time of 6—7 min. The heat capacity curve exhibited a step-like anomaly at this temperature. The heat capacity value could not be defined precisely in this temperature region, because it depended on the annealing condition of the sample and on the time spent in the measurement. Another anomaly was found at around 218 K which corresponds to the phase transition temperature reported by Kiriyama.[3] The equilibration time did not change appreciably around the transition point. At still higher temperature a broad hump was found, which could be attributed to the eutectic melting due to the presence of the excess water. The cell was dismantled from the cryostat and the excess water was carefully removed. Subsequent measurement showed the broad hump was absent, though the first two anomalies remained unaffected. Since the relaxational anomaly mentioned above was quite unexpected, it was suspected that it might be caused by impurity in the sample crystal. The extremely pure crystal was prepared as was mentioned above. The measurement on the improved specimen yielded the same result in regard to the relaxational and the lambda anomalies. Therefore it was concluded that the first two anomalies are intrinsic properties of the crystal. Since different cooling history of the sample was found to cause change in the behavior of the crystal, a detailed measurement was attempted which enabled a quantitative analysis of the hysteretic phenomenon under controlled condition. The procedure was as follows. The calorimeter was cooled through the anomalous region as rapidly as possible to 133 K, at which temperature a series of measurement was started in the usual intermittent heating mode with the temperature step of 1—1.5 K. At 138.1 K a significant heat evolution began. The temperature rose linearly with time, indicating that the relaxational effect involved is a slow process. After following the temperature drift for 30 min, the temperature was raised by about 1 K by introducing the electric energy in the calorimeter and again the temperature rise was followed for 30 min. The same procedure was repeated to above 160 K. The rate of the spontaneous temperature rise reached its maximum at 149.5 K, above which it decreased rapidly, reaching null approximately at 154 K. Above 154 K, the temperature drift after turning-off of the heater current was endothermic and non-linear in time. The linear exothermic drift rate at the lower temperatures is plotted in Fig. 1 as a function of the temperature. A similar behavior was observed in the deuterate crystal. As is

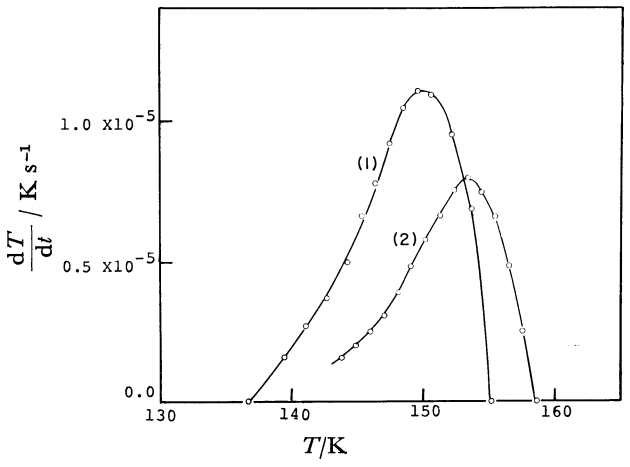

Fig. 1. Rate of spontaneous temperature rise of the calorimeter loaded with (1) $SnCl_2 \cdot 2H_2O$ and (2) $SnCl_2 \cdot 2D_2O$.

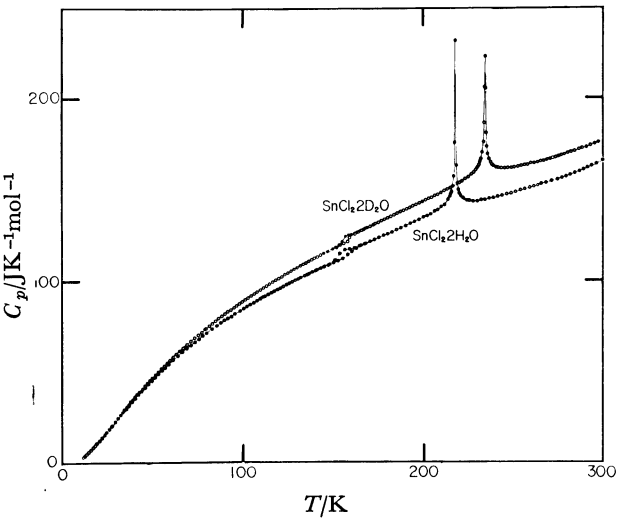

Fig. 2. Heat capacity of $SnCl_2 \cdot 2H_2O$ and $SnCl_2 \cdot 2D_2O$ crystals.

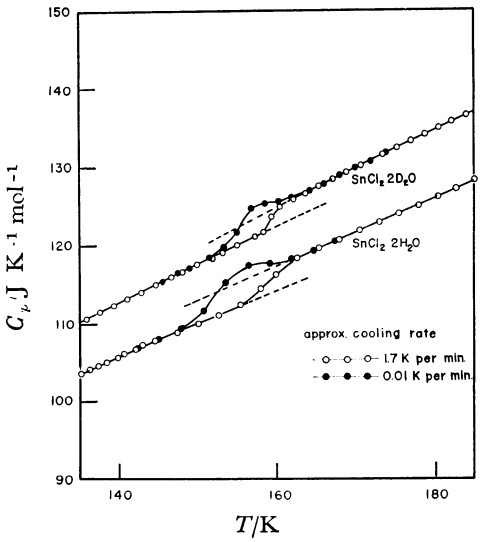

Fig. 3. Heat capacity of $SnCl_2 \cdot 2H_2O$ and $SnCl_2 \cdot 2D_2O$ around their "glass transition" temperatures. Because of spontaneous heat evolution and other non-equilibrium phenomenon, some arbitrariness is necessarily introduced to the observed values. The effect of different sample prehistory is indicated by the open and closed circles in the plot. Measurement after rapid cooling (1.7 K per min) gave the smaller values (open circles), and after slow cooling (0.01 K per min), the larger value (closed circles) in the temperature region 150—163 K.

TABLE 1. HEAT CAPACITY OF $SnCl_2 \cdot 2H_2O$

T / K	C_p / J K^{-1} mol^{-1}	T / K	C_p / J K^{-1} mol^{-1}	T / K	C_p / J K^{-1} mol^{-1}	T / K	C_p / J K^{-1} mol^{-1}
79.53	72.58	140.63	107.10	223.5865	145.91	149.51	112.73
82.57	74.91	142.85	108.19	224.99	145.39	151.79	115.14
85.19	76.80			227.01	145.06	154.04	116.93
87.38	78.41	142.05	107.67	229.23	145.06	156.28	117.43
89.46	79.75	144.54	108.77			158.50	117.51
91.26	80.81	147.28	109.95	79.49	72.46	160.71	118.54
93.28	82.15	149.98	111.08	81.62	74.05	162.91	119.26
95.26	83.31	152.66	111.64	84.93	76.47	165.09	120.28
98.02	85.00	155.31	113.55	89.00	79.31	167.26	121.15
99.92	86.15	157.90	115.77				
101.81	87.23	160.45	117.45	109.97	91.65	172.27	123.70
103.66	88.32	162.97	119.24	112.65	93.04	174.79	124.57
105.49	89.37	165.49	120.75	116.97	95.84	177.35	125.23
107.30	90.37	167.99	121.85	119.78	96.74	179.94	126.82
109.10	91.39	170.47	122.94	122.54	98.30	182.50	127.95
110.87	92.30			125.27	99.55	185.05	129.07
		299.72	166.86	127.96	100.89	187.59	130.08
11.70	3.85	301.18	168.54	130.61	102.16	190.10	131.28
12.60	4.49			133.23	103.40	192.60	132.44
13.67	5.46	153.82	112.55	136.37	104.85	195.07	133.58
14.82	6.68	155.06	112.95	138.92	105.91	197.53	134.67
15.99	7.69	156.29	114.29	141.25	107.13	199.96	135.94
17.23	9.19	157.49	116.42	143.95	108.19		
18.39	10.45	158.69	117.60	146.43	109.34	228.35	145.00
19.46	11.72	159.85	118.46	148.89	110.72	230.76	145.10
20.72	13.12	161.27	118.19			233.17	145.42
22.07	14.80	162.40	119.30	213.92	145.84	235.55	145.78
23.36	16.26			215.3419	148.49	237.93	146.38
24.61	17.60	182.53	127.88	215.5982	149.07	240.28	146.88
26.08	19.50	183.59	128.64	215.8218	149.62	242.62	147.33
27.72	21.48			216.0444	150.27	244.95	147.70
29.34	23.40	267.71	154.33	216.2663	151.34	247.26	148.32
30.94	25.34	270.11	154.84	216.4872	152.13		
32.42	27.06	272.49	155.68	216.7430	153.92	249.58	148.87
33.79	28.71	274.89	156.82	216.9978	155.83	252.01	149.52
35.22	30.45	277.25	157.38	217.2142	158.02	254.44	150.22
36.72	32.23	279.62	157.99	217.4262	162.79	256.85	150.93
38.46	34.22	281.96	158.89	217.6335	168.80	259.25	151.75
40.42	36.38	284.31	159.85	217.8223	210.90	261.64	152.56
42.24	38.41	286.63	161.09	217.9418	651.25	264.03	153.15
43.96	40.27	288.94	161.89	218.0718	181.05	266.41	153.80
45.76	42.22	291.25	162.66	218.2724	166.20	268.78	154.43
47.65	44.28	293.54	163.74	218.4822	159.55		
49.45	46.09			218.6964	156.92	135.79	104.01
51.32	48.15	203.38	137.71	218.9131	154.88	137.51	105.03
53.27	50.04	205.49	138.92	219.1307	153.97	140.32	106.56
55.14	51.79	208.62	140.90	219.3517	151.86		
56.93	53.48	211.93	143.44	219.5735	151.45	135.91	104.61
58.84	55.39	213.7628	145.70	219.7905	150.00	138.07	105.70
61.20	57.61	214.6714	146.95	220.0183	149.15	140.22	106.84
63.79	60.00	215.2727	148.32	220.3162	149.20	141.81	107.46
66.26	62.11	215.8690	149.66	220.7256	148.04	143.40	108.10
68.64	64.08	216.4597	152.27	221.2508	147.51	144.73	108.67
70.94	65.91	217.0417	156.35	221.9034	146.91	145.73	107.83
73.18	67.62	217.5987	171.73	222.7868	146.11	146.84	109.67
75.35	69.36	218.0552	171.79	224.0270	145.59	147.89	110.12
77.46	71.00	219.1017	153.29	225.4467	145.24	148.95	110.49
		219.6889	150.80	226.8681	145.01	150.00	111.02
129.95	102.15	220.2818	149.11	228.2901	144.93	151.30	111.20
131.91	103.03	220.8738	148.21			152.85	112.15
133.86	104.01	221.4777	147.00	142.42	107.62	155.13	112.66
136.14	105.01	222.0787	146.64	144.81	108.68	156.12	115.60
138.39	105.73	222.6813	146.06	147.18	109.94	165.84	119.63

TABLE 2. HEAT CAPACITY OF $SnCl_2 \cdot 2D_2O$

T/K	C_p/J K^{-1} mol^{-1}	T/K	C_p/J K^{-1} mol^{-1}	T/K	C_p/J K^{-1} mol^{-1}	T/K	C_p/J K^{-1} mol^{-1}
241.75	162.82	112.71	98.17	220.10	154.74	238.0153	165.13
243.58	162.74	114.41	99.20	221.62	155.61	238.1902	164.75
245.41	162.59	116.09	100.23	223.28	156.82	238.3657	164.51
247.24	162.64	117.76	101.24	225.02	157.90	238.5407	164.14
249.07	162.88	119.41	102.23	226.77	159.37	238.7162	164.35
250.90	163.04	121.09	103.25	228.22	160.77	238.8916	163.83
252.72	163.46	122.85	104.23	229.23	161.69	239.0670	164.39
254.54	164.03	124.61	105.17	229.80	163.00	239.2425	163.82
256.37	164.47	126.37	106.26			239.4283	163.77
258.17	164.63	128.10	107.25	226.5014	158.89	239.5937	164.18
259.97	165.36	129.82	108.22	227.1171	159.64	239.7693	163.39
261.78	165.34	131.53	109.15	227.6538	159.83	239.9450	163.87
263.58	165.79	133.22	110.07	228.1974	160.36	240.2086	163.54
265.38	166.34	134.58	110.84	228.7389	161.20	240.5605	163.16
267.18	166.59	136.26	111.69	229.2787	161.63	240.9710	163.40
268.96	167.28	137.88	112.55	229.7203	162.38	241.4400	163.33
270.77	167.76	139.43	113.38	229.9785	162.79	241.9019	163.06
272.60	168.43	141.04	114.22	230.1502	163.12		
		142.76	115.01	230.3219	162.92	141.10	114.23
288.34	173.62	144.52	115.93	230.4936	163.35	142.16	114.44
290.61	174.26	146.25	116.78	230.6648	164.09	143.22	115.31
292.88	175.20	147.97	117.65	230.8358	164.04	144.30	115.88
295.15	176.11	149.67	118.49	231.0067	164.47	145.37	116.51
297.40	177.27	151.39	119.45	231.1774	164.57	146.43	116.94
		153.14	120.79	231.3478	165.27	147.50	117.60
227.79	160.23	154.89	122.58	231.5177	165.68	148.56	118.11
229.74	162.63	156.61	125.57	231.6874	166.03	149.62	118.47
231.67	166.53	158.30	126.29	231.8567	166.82	150.68	119.21
233.51	182.51	159.97	126.52	232.0256	166.84	151.74	119.32
235.28	185.22	161.68	127.17	232.1967	167.74	152.81	119.87
237.11	166.99	163.44	127.65	232.3695	168.36	153.86	120.51
239.01	164.43	165.19	128.58	232.5419	169.12	154.92	120.97
240.93	163.49	166.92	129.40	232.7162	170.22	155.96	121.53
		168.68	130.31	232.8924	171.30	156.99	122.05
273.87	169.43	170.45	131.07	233.0684	171.79	158.02	122.67
275.78	169.86	172.24	131.88	233.2437	173.39	159.02	124.90
277.68	170.49	173.29	132.40	233.4173	175.12	160.27	125.93
279.57	171.17	175.03	133.25	233.5893	177.65	162.00	126.84
281.47	171.84	176.77	134.09	233.7591	181.26	163.97	127.97
283.35	172.49	178.50	134.91	233.9234	187.72	165.92	128.86
285.23	173.04	180.22	135.72	234.0884	192.73	167.86	129.96
287.10	173.79	181.92	136.53	234.2453	207.30	169.79	130.89
		183.66	137.38	234.3985	223.19	171.70	131.56
79.34	74.87	185.41	138.19	234.5443	223.92	173.61	132.63
81.14	76.36	187.16	138.98	234.6973	206.45		
82.91	77.79	188.90	139.77	234.8599	190.82	11.90	3.89
84.64	79.18	190.63	140.55	235.0301	182.36	12.87	4.49
86.35	80.57	192.35	141.35	235.2049	177.45	13.81	5.63
88.06	81.87	194.06	142.22	235.3824	174.69	14.73	6.58
89.74	83.08	195.80	142.96	235.5619	172.69	15.69	7.55
91.39	84.21	197.55	143.84	235.7400	171.18	16.69	8.69
93.02	85.32	199.30	144.45	235.9159	170.42	17.66	9.70
94.62	86.38	201.04	145.44	236.0924	169.39	18.56	10.84
96.22	87.51	202.78	146.15	236.2697	168.54	19.68	11.93
97.82	88.23	204.50	146.92	236.4474	168.07	20.62	13.16
99.40	89.63	206.24	147.82	236.6228	167.43	21.47	14.12
100.96	90.68	208.01	148.48	236.7959	167.07	22.42	15.30
102.51	91.70	209.78	149.43	236.9693	167.06	23.55	16.68
104.17	92.73	211.53	150.35	237.1430	166.07	24.69	18.07
105.91	93.93	213.28	151.17	237.3171	166.19	25.74	19.31
107.63	94.99	215.01	152.09	237.4912	165.94	26.79	20.70
109.34	96.08	216.74	152.85	237.6757	165.20	27.85	21.99
111.02	97.09	218.49	153.83	237.8405	165.29	29.13	23.53

Table 2. (Continued)

T/K	C_p/J K^{-1} mol^{-1}	T/K	C_p/J K^{-1} mol^{-1}	T/K	C_p/J K^{-1} mol^{-1}	T/K	C_p/J K^{-1} mol^{-1}
30.60	25.35	61.12	59.00	230.5518	164.24	235.3367	175.76
31.95	27.08	62.98	60.81	230.7832	164.68	235.5574	173.17
33.22	28.64	64.78	62.50	231.0143	164.73	235.7800	171.59
34.43	29.99	66.78	64.28	231.2451	165.20	236.0037	170.59
35.57	31.50	68.96	66.14	231.4752	166.05	236.2286	169.39
36.79	32.94	71.07	67.94	231.7044	166.31	236.4546	168.46
37.96	34.30	73.13	69.69	231.9329	167.38	236.6809	168.40
39.07	35.59	75.13	71.35	232.1605	168.32	236.9077	167.31
40.25	36.96	77.07	72.98	232.3871	169.06	237.1352	166.79
41.38	38.26	78.98	74.55	232.6129	169.90	237.3635	166.60
42.71	39.83	80.84	76.13	232.8377	171.04	237.5913	165.63
44.24	41.42	82.66	77.62	233.0612	172.64	237.8201	165.64
45.70	43.08			233.2831	174.40	238.0490	165.37
47.10	44.58	74.78	71.09	233.5032	176.81	238.2780	165.34
48.44	46.14	77.46	73.54	233.7200	181.24	237.5073	164.68
49.86	47.62	80.25	75.62	233.9324	186.90	238.7369	164.82
51.48	49.32			234.1378	198.64	238.9665	164.53
53.19	51.07	229.4506	162.03	234.3319	217.24	239.1961	164.85
54.83	52.75	229.6621	162.76	234.5167	225.71	239.4257	164.57
56.42	54.32	229.8823	162.81	234.7053	206.22	239.6554	164.68
57.95	55.86	230.1015	163.41	234.9073	188.27	239.8857	163.01
59.44	57.35	230.3234	163.43	235.1193	180.63		

shown in the figure the anomaly occurred in the deuterate at somewhat higher temperature. An analysis of the observed effect will be given in the later section.

After measuring the heat capacity for the entire temperature region, the transition region was investigated in more detail. The temperature increment for one step of measurement was 0.007—0.23 K, compared to 1—3 K for the normal region. The observed heat capacity was 10 times as large as the normal heat capacity at the peak, but no latent heat was observed.

Experimental Results. The heat capacity curves for the entire temperature region are shown in Fig. 2. The numerical values are given in Tables I and II. The lambda peaks at 218 K and 235 K are nearly symmetrical in shape with respect to the respective peak temperature. In Fig. 3, the anomalies around 150 K are represented in an expanded scale. The open circles correspond to the quenched sample and the filled circles to the annealed. Similar curves for the deuterate are also shown in the figure. As was stated earlier, the *endo-* and *exo-*thermic effects made it difficult to determine unambiguously the heat capacity around the temperature. The values plotted in the figure are those calculated by employing the temperatures extrapolated to the mid-point of the heat-on period in case of the linear exothermic drifts. In the endothermic case, the temperatures observed at 30 minutes after the heat input interval were taken as the final temperatures. This convention of the data reduction is arbitrarily adopted.

General feature of the heat capacity curve and the enthalpy relaxation observed around this temperature are quite similar to those reported in a number of glass forming substances including the glassy crystals.[4] However, the heat capacity jump (2—3 J K^{-1}mol^{-1}) is considerably smaller than is usual in a glassy crystal (30—50 J K^{-1}mol^{-1}). Absence of any effects attributable to crystallization is also in clear contrast to the typical behavior of the glassy state formed by low molecular-weight substances. As will be discussed later in more detail, the newly found non-equilibrium state may be regarded as a new type of glassy states in which incompletely long-range-ordered proton (or deuteron) configuration is frozen in the immobile state.

Discussion

The Relaxational Anomaly. In order to derive physically informative parameters from the heat evolution rate observed around 150 K, the heat evolution rate given in Fig. 1 was integrated numerically with time, to give the enthalpy-temperature relation shown in Fig. 4, where the configurational enthalpy was separated from the rest by taking the low temperature

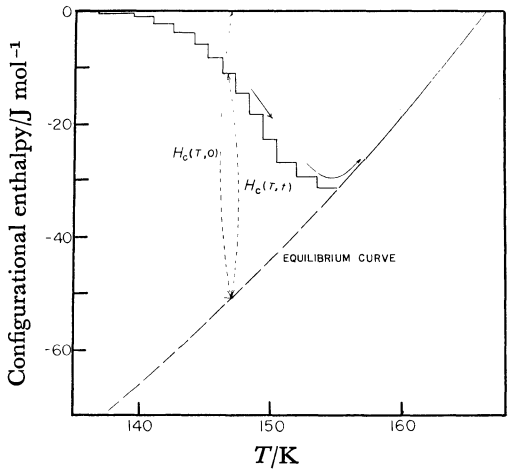

Fig. 4. Temperature-configurational enthalpy relation of $SnCl_2 \cdot 2H_2O$ crystal around its "glass transition" temperature. The arrows indicate the path followed by the crystal in this particular measurement. $H_c(T_0,)$ and $H_c(T,t)$ is the variables in the rate equation given in the text. The equilibrium curve below 155 K is calculated from the extrapolated configurational heat capacity.

heat capacity as the back-ground contribution. The reference temperature was chosen arbitrarily as $T_0=$ 166.50 K for the hydrate. The equilibrium curve was calculated by integrating numerically the difference between the extrapolated high temperature heat capacity and the low temperature one. The zig-zag chain in Fig. 4 is the path whicn the configurational enthalpy followed as the crystal was warmed after rapid cooling. A similar zig-zag curve was obtained for the deuterate. Decrease of the enthalpy with increasing temperature indicates, of course, that the process is not a thermodynamically equilibrium one. Moreover, the enthalpy-temperature relation shown by the curve is not a unique representation of the property of the crystal, but depends on the thermal history of the crystal, particularily on the cooling rate and the time spent on the measurement. The nearly horizontal segments in the curve correspond to the heat-on period, while the nearly vertical segments to the drift period. From the observed drift rates, the relaxation time was evaluated as follows. If an exponential law is assumed for the approach to the equilibrium configuration, the rate law can be written as follows:

$$\frac{dH(T,t)}{dt} = -\frac{H(T,t)}{\tau} \qquad (1)$$

where $H(T,t)$ is the configurational enthalpy referred to the equilibrium value at temperature T and time t and τ the relaxation time. The left-hand side of Eq. (1) is related to the temperature drift rate dT/dt by the equation:

$$\frac{dH(T,t)}{dt} = -C\frac{dT}{dt}, \qquad (2)$$

where C is the heat capacity of the cell containing the sample crystal. Combining the Eqs. (1) and (2), one obtains:

$$\tau = \frac{H(T,t)}{C\dfrac{dT}{dt}} \qquad (3)$$

By taking $H(T,t)$ from Fig. 4 and C and dT/dt from the experimental values, the relaxation time could be evaluated as a function of temperature. The heat capacity C is not defined around this temperature but the fraction of the ambiguous portion is small compared with the total heat capactiy. The calculated τ is affected little by the ambiguity in the estimation of the heat capacity value. The relaxation time thus evaluated is shown in Fig. 5 as an Arrhenius plot. It is remarkable that the drift rate *vs.* temperature curves in Fig. 1 could be reduced to the straight lines in Fig. 5. The lines were least-square-fitted to a linear equation from which the activation energies were estimated to be 49.88 ± 0.33 and 49.78 ± 0.23 kJ mol^{-1} for the hydrate and the deuterate, respectively. The frequency factors evaluated are $(1.92\pm0.6)\times10^{13}$ and $(0.5\pm0.2)\times10^{13}$ Hz. The derived activation energies are significantly smaller than that obtained by Kiriyama from the temperature dependence of the DC conductivity (17 kcal mol$^{-1}\cong$71 kJ mol^{-1}). This may simply mean that the mechanisms involved in the two dissipative processes are different from each other. The DC conduction is caused by transportation of the ionic species in the crystal. On the other hand, the enthalpy relaxation can proceed without involving ionic species, so that the two activation energies should not necessarily be equal to each other. The activation energy, 49.8 kJ mol^{-1}, is twice as large as the typical hydrogen bond energy of O–H···O system. Molecular interpretation of this value seems to be complicated as is explained in the following.

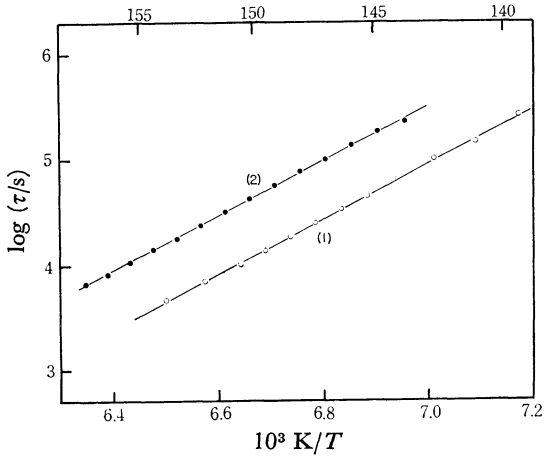

Fig. 5. Arrhenius plot of the enthalpy relaxation time τ of (1) $SnCl_2\cdot2H_2O$ and (2) $SnCl_2\cdot2D_2O$.

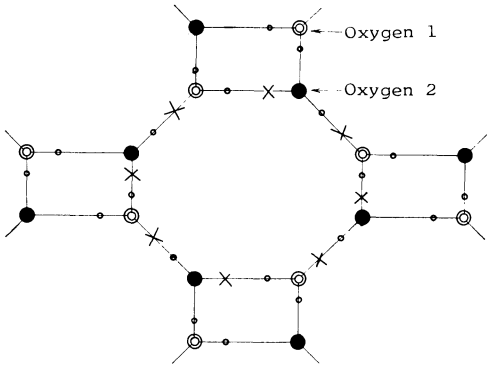

Fig. 6. Schematic diagram of the hydrogen bond network of $SnCl_2\cdot2H_2O$ and $SnCl_2\cdot2D_2O$. Oxygens 1 indicated by the double circles have two mobile hydrogen (or deuterium) atoms, while Oxygens 2 indicated by the closed circles have one mobile hydrogen and one immobile hydrogen. The latter not shown in the figure is hydrogen bonded to the chlorine atom. The small circles indicate the perfectly ordered hydrogen positions. The set of the eight crosses is the smallest unit by which the network deviates from the perfect order if the ice condition is imposed.

The hydrogen position determined by neutron diffraction[2] is described schematically in Fig. 6. This corresponds to the perfectly ordered situation, which could never be attained in the usual experimental time scale. But as is revealed in the configurational entropy diagram (Fig. 7) constructed by integrating the extrapolated anomalous heat capacity curve, the residual disorder retained in the real crystal is so small that the hydrogen position given by the diffrac-

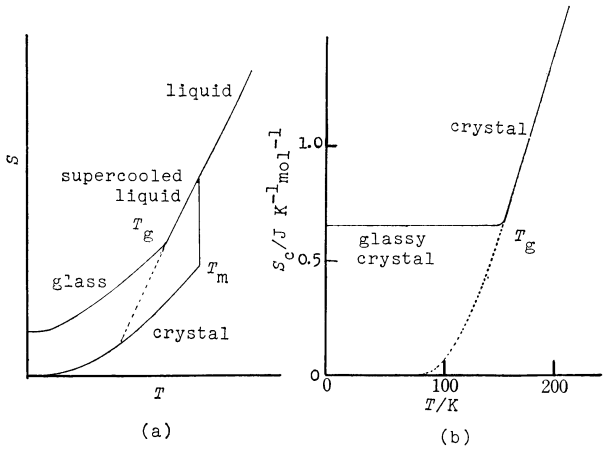

Fig. 7. Entropy of the glass-forming systems.
(a) Entropy of a typical substance forming a crystal, liquid and glass.
(b) Configurational entropy of $SnCl_2 \cdot 2H_2O$ crysatl retaining a small residual entropy ($\sim$0.65 J K^{-1} mol^{-1}). The broken portion of the curve is calculated from the extrapolated configurational heat capacity.

tion method and the weight assigned to each position are essentially those of the perfectly ordered crystal. Now, careful examination of this figure shows that if the ice condition is to be satisfied the smallest unit that can deviate from the perfect order is the eight-membered ring. The crosses in the figure indicate the position which the hydrogen atoms occupy in the locally disordered state. If this disordered state tries to approach the perfect order, the eight hydrogen atoms had to move in unison, so that the activation energy would be eight times as large as is needed to break one hydrogen bond, or 25 kJ mol^{-1} $\times$ 8 = 200 kJ mol^{-1}. This is about four times as large as the experimental value. This seems to mean that some defect mechanism has to be invoked. Possibly, Bjerrum defects (D and L) take part in the reorientation process causing change of the order parameter.

It should be added here that the residual entropy indicated in Fig. 7 is an apparent one, since it is not based on equilibrium measurements but was simply calculated from the extrapolated heat capacity data. But it is believed to be close to the correct value because the structural data indicate that the crystal retains no other disorder than that of the hydrogen position.

In closing the discussion of the relaxational anomaly, relation of the present observation to the widely observed glass transitions is discussed. In addition to the widely-known polymeric glass-forming materials, a number of substances composed of relatively simple molecules were found to form glassy states.[4] The glassy states are classified into the glassy liquids, glassy crystals and glassy liquid crystals according to the type of disorder that is brought into the non-equilibrium state. In the first both the molecular position and molecular orientation are at random and do not possess long range periodicity. In the second the position is regular but the random orientation of the molecules is frozen in, and in the third, the positional disorder is retained, while the molecular orientation is in the ordered state. In stannous chloride dihydrate, the heavy atom positions are ordered and the hydrogen positions are nearly ordered, as is suggested by the entropy diagram (Fig. 7). It is, therefore, appropriate to classify it into a new type of glassy crystal in which the frozen-in degree of freedom has a long range order. Although there have not been examples of this kind reported so far, there seems to be nothing unnatural in the concept of the long-range-ordered glassy state. An important qualitative consequence is that a substance in this non-equilibrium state will not be induced to crystallize; only the long range order develops further without any discontinuous change of the crystal symmetry or other properties of the substance. This is one of the reasons why the relaxational effect could be investigated in detail to enable evaluation of the activation energy precisely.

Origin of the variety of the glassy states mentioned above can be traced back to the relation of the transition temperature and the temperature dependence of the molecular relaxation time. Here, the transition temperature means the temperature at which a long range order begins to develop in the (high-temperature) disordered degree of freedom of the substance. Temperature dependence of the order parameter is different from substance to substance. It may develop abruptly as in the first-order transitions (*e.g.* crystallization or transitions from plastic to non-plastic crystals). More gradual changes are typically observed in lambda anomalies in a number of order-disorder transitions. The molecular relaxation time, on the other hand, depends primarily on the barrier height which the molecules have to overcome if they are to reorient or to be redistributed in the substance. It increases generally rapidly with decreasing temperature, sometimes accompanied by a discontinuous change at transition temperatures. The ratio of the relaxation time to the experimental observation time is called the Deborah number[6] by Rheologists. By using the concept of Deborah number, the glassy state can conveniently be classified, together with other equilibrium and non-equilibrium states.

If the Deborah number of a substance is already large at high enough temperatures as compared to the hypothetical transition temperature, no relaxational effects will be observed thermally. This may be the case of CO, NO, or N_2O crystals. These crystals have residual entropies at 0 K[7] and are not known to exhibit thermal relaxation. In ice and heavy ice, for which the residual entropy has been discussed long, a small relaxational anomaly was recently discovered calorimetrically.[8,9] The temperatures at which the anomaly occurs are 95 and 105 K for the ordinary ice and heavy ice, respectively. It was proposed that the Deborah number happens to approach unity at the temperatures where the short range order of the proton configuration in the ice crystals begins to develop.

Next, if the Deborah number becomes unity at the temperature where the long range order is present but not complete, the relaxational effect will again be observed. This is what happens in the present case

of stannous chloride dihydrate. Finally if the ordering is already completed before the Deborah number approaches unity, no relaxational phenomena will be observed. This is the case for a number of substances for which the third law of thermodynamics is verified experimentally.

The variety of experimental observations could thus be classified according to the relative magnitude of the (in some cases, hypothetical) transition temperature and the temperature at which calorimetric Deborah number becomes unity.

The Phase Transition. The gradual anomaly at 218 K is due to the order-disorder transition of the hydrogen position. A similar anomaly occurs at 235 K in the deuterate. Structurally these are antiferroelectric to paraelectric transitions, as was shown by Kiriyama by use of magnetic resonance, X ray and neutron diffraction methods.[2] Although the heat capacity peak at 218 K is relatively narrow the outskirt region is extended over a wide temperature range. In fact, according to the interpretation of the relaxational anomaly discussed in the last section, the anomalous contribution is appreciable even at 150 K. The total entropy change is, therefore, difficult to estimate with certainty. In order to minimize arbitrariness, heat capacity of barium chloride dihydrate[10] was compared with the present heat capacity curve. This crystal has a similar layer structure and, moreover, its molecular weight is very close to that of stannous chloride dihydrate. Since barium chloride dihydrate does not show heat capacity anomaly below room temperature, it was expected to serve as a reference material. The heat capacity is a smooth function of temperature, and slightly smaller than that of stannous chloride dihydrate at 260 K. The normal heat capacity of stannous chloride dihydrate was assumed by joining the $BaCl_2 \cdot 2H_2O$ value at 260 K and the $SnCl_2 \cdot 2H_2O$ value at 150 K with a smooth curve. The anomalous part above 260 K was assumed to follow the T^{-2} law, as is expected for any interacting systems by a high temperature expansion. The low temperature contribution which could not be measured because of the long relaxation time was calculated from the extrapolated heat capacity curve. The total entropy change thus estimated is 4.6 J K^{-1} mol^{-1}, for the both crystals. Rigorous theoretical value given in the appendix is 3.13 J K^{-1} mol^{-1}. It is probable that the high temperature contribution to the estimated experimental value might be too large and also that other degrees of freedom than the hydrogen configuration would be contributing significantly to the observed transition entropy. Since the base line determination introduces a large uncertaintyin to the experimental value, detailed discussion of these values would be difficult at present.

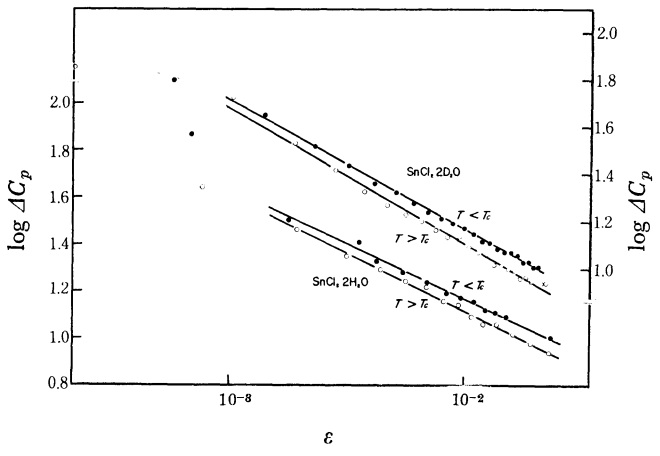

Fig. 8. Logarithmic plot of the anomalous part of the heat capacity of $SnCl_2 \cdot 2H_2O$ and $SnCl_2 \cdot 2D_2O$.

In the vicinity of the lambda transition the heat capacity diverges as is shown in Fig. 2. There has been discussion on the types of the singularity of the heat capacity curves at ferroelectric transitions. For the antiferroelectrics, there seems to be relatively fewer examples. It has been conjectured that the effect of domain formation and of finite crystal size would affect the critical behavior of the ferroelectric crystals. Such effects will be absent or at least relatively unimportant in antiferroelectrics. It is hoped that the present crystal would provide an ideal system to study the critical behaviors on. The anomalous heat capacity is plotted in Fig. 8 in a logarithmic scale, which, at least for $\varepsilon = |(T - T_c)/T_c| > 10^{-3}$, is linear, indicating that

$$\Delta C = A_{\pm} |(T - T_c)/T_c|^{-\alpha_{\pm}}$$

where $\alpha_{\pm}$ are given in Table 3. Attempts were made to fit the data to

$$\Delta C = A_{\pm} \ln |(T - T_c)/T_c|$$

But no good fits were obtained. Any possible change of the normal heat capacity does not alter the conclusion. It should be added that the calorimeter used was not entirely suitable for the high resolution measurement, so that the important region of $\varepsilon < 10^{-3}$ was missed. A high resolution calorimeter capable of the temperature resolution smaller than 10^{-5} K was constructed. Heat capacity measurement with the new apparatus was performed on a single crystal of $SnCl_2 \cdot 2H_2O$ in the close vicinity of the critical temperature. The result will be reported soon in a separate publication.

Table 3.

	$SnCl_2 \cdot 2H_2O$	$SnCl_2 \cdot 2D_2O$
T_c/K	217.94 ±0.05	234.47±0.05
α_+	0.534±0.021	0.574±0.010
α_-	0.478±0.010	0.544±0.010

The error bounds assigned to the α values refer to the scattering of the data about the linear plot. If the ambiguity in the estimation of the normal heat capacity is taken into account, they will be somewhat larger.

Finally, the thermal behavior of the present crystal is compared with that of other hydrate crystals. Copper formate tetrahydrate and its deuterate analogue have a similar layer structure, in which the water molecules form a hydrogen-bonded network.[11-14] The

† T. Matsuo, H. Suga, and S. Seki, unpublished work.

hydrogen position in the water layer exhibits an order-disorder transition to an antiferroelectric state. The heat capacity has a sharp peak at 236 K and at 246 K for the hydrate and the deuterate,† respectively. The molar volume changes abruptly at the transition, indicating that the phase transition is of the first order. Potassium ferrocyanide trihydrate and trideuterate,[15] also layer structure compounds,[16,17] undergo a ferroelectric transition at 248 and 253 K, respectively. The ferroelectricity is believed to originate from the alignment of the water molecules in the hydrogen-bonded layers. The heat capacity anomaly does not tend to infinity but remains finite. There is a finite jump in the heat capacity and the thermal expansion coefficient.[15] These jumps were found to satisfy the Ehrenfest relation for the pressure dependence of the second-order phase transition temperature. One has to conclude that inspite of the structural similarity of these hydrate crystals, their critical behaviors are quite disparate from each other.

It may be added that structural investigations have shown that below the critical points the three-dimensional order begins to develop in these crystals, despite the two-dimensional character of the crystal structures. However, contrary to magnetic cases where development of the magnetic spin correlation are studied in close vicinity of the Curie (or Néel) temperature,[18] no such attempt seems to have been reported for the ferro- and antiferro-electric substances having layer structure. It would be of interest to study such effects in the present substances.

Appendix:‡ High Temperature Entropy Calculation by J. F. Nagle

In this appendix the high temperature (completely disordered) entropy is calculated. The first step in the calculation is to establish an isomorphism between this hydrogen bonded problem and a dimer problem. Consider a configuration of protons on the $SnCl_2 \cdot 2H_2O$ lattice shown in Fig. 6 of the text. Half of the oxygen atoms O(2), namely those on sublattice, A, each have one immobilized proton and one mobile proton. The other half of the oxygen atoms O(1), namely those on the other sublattice B, which interpenetrates sublattice A, each have two mobile protons. Given a configuration of protons let one third of the bonds be distinguished, *i.e.* made into dimers. Those bonds which are distinguished are the ones which have a proton near the oxygen atoms on sublattice A. These bonds join oxygen atoms in pairs and each oxygen atom is paired to precisely one other oxygen atom. By definition such a state is a close packed dimer state. Each proton configuration defines a unique close-packed dimer state and each dimer state defines a unique proton state so the correspondence is one to one.

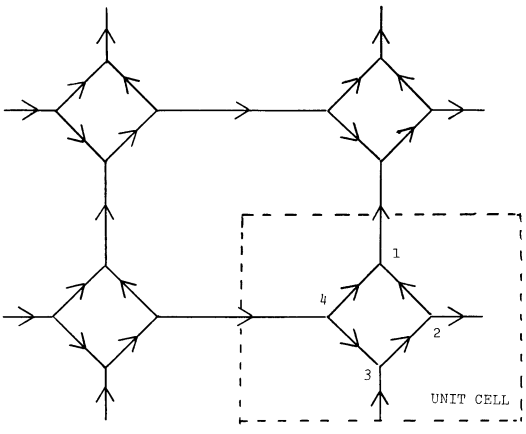

Fig. A1. The hydrogen bond network of $SnCl_2 \cdot 2H_2O$. The set of arrows satisfies Kasteleijn's "clockwise odd" rule and determines the signs in $M(\phi_1, \phi_2)$.

The next step is to follow Kasteleijn's method[19] of solving dimer problems. This step is quite well known.[20] One finds a "clockwise odd" arrangement of arrows as shown in Fig. A1. which then determines the signs of the elements entering the Pfaffian which is then the square root of a cyclic determinant which can be reduced to products of determinants of the following form:

$$M(\phi_1, \phi_2) = \begin{pmatrix} 0 & -1 & e^{i\phi_2} & -1 \\ 1 & 0 & -1 & e^{i\phi_1} \\ -e^{-i\phi_2} & 1 & 0 & -1 \\ 1 & -e^{-i\phi_1} & 1 & 0 \end{pmatrix}$$

The partition function per molecule of $SnCl_2 \cdot 2H_2O$ is then

$$\frac{\ln Z}{N} = \left(\frac{1}{4\pi}\right)^2 \int_0^{2\pi}\int_0^{2\pi} \ln\,[\det M(\phi_1, \phi_2)]\,d\phi_1 d\phi_2$$

$$= \left(\frac{1}{4\pi}\right)^2 \int_0^{2\pi}\int_0^{2\pi} \ln\,[5 - 4\cos\phi_1 \cos\phi_2]\,d\phi_2 d\phi_2$$

Since the internal energy is zero, the entropy is just $S/R = (\ln Z)/N$.

The last step is to evaluate this integral and this has been done in two ways. The pedestrian way is to expand $\ln[1 - (4/5)\cos\phi_1 \cos\phi_2]$ and integrate term by term, giving

$$\frac{S}{R} = \frac{1}{4}\ln 5 - \frac{1}{4}\sum_{n=1}^{\infty} \frac{(4/5)^{2n}}{2n}\left[\frac{1 \cdot 3 \cdots (2n-1)}{2 \cdot 4 \cdots 2n}\right]^2.$$

Calculation by computer of twenty terms in the series give 7 significant figures and 100 terms gives 24 significant figures as shown by computing obvious upper bounds on the remainder of the series. The second way to evaluate the integral is to realize that the double integral has the same form as the integral for the square lattice Ising model, which is not surprising in view of the similarity of the lattice used for the dimer solution of the square lattice Ising model[19] and the lattice of Fig. A1. Then, one can use the rapidly converging series developed by Onsager.[21] Only seven terms in Onsager's series are required for 15 significant figures.

The final result to 15 significant figures is

$$S/R = 0.376995650569878\cdots$$

This model is amenable to extension to finite temperatures which will provide detailed comparison with specific heat measurements and NMR or neutron determination of deuteron or proton occupational probabilities. This work is in progress.

The authors are indebted to Professors Ryoichi

‡ The result of this appendix was reported as a discussion comment by J. F. Nagle following the paper by T. Matsuo *et al.* in the Proceedings of the International Symposium of the Physics and Chemistry of Ice, Ottawa, 1972, to be published by the Royal Society of Canada.

Kiriyama and Hideko Kiriyama for the fruitful discussion on the crystal structure and for making their unpublished structural data available to them. Contributions of the former students at the laboratory, Mr. Yasushi Miyoshi, now at Sanyo Electric Co. and Mr. Koji Kitamura, now at Kyoto University, were substantial at the early stage of the experiment, to whom the authors are grateful.

References

1) B. Kamenar and D. Grdenic, *J. Chem. Soc.*, **1961**, 3957.
2) H. Kiriyama, K. Kitahama, O. Nakamura, and R. Kiriyama, This Bulletin, **46**, 1389 (1973); *Acta Crystallogr.*, **A28**, S240 (1972).
3) H. Kiriyama and R. Kiriyama, *J. Phys. Soc. Japan*, **28**, Suppl., 114 (1970).
4) K. Adachi, H. Suga, and S. Seki, This Bulletin, **41**, 1073 (1968); **43**, 1916 (1970); **44**, 78 (1971).
5) T. Matsuo, H. Suga, and S. Seki, *J. Phys. Soc. Japan*, **30**, 785 (1971).
6) M. Reiner, *Physics Today*, **17**, (1), 62 (1964).
7) J. Wilks, The Third Law of thermodynamics," Oxford University Press, London and New York (1967).
8) O. Haida, T. Matsuo, H. Suga, and S. Seki, *Proc. Japan Acad.*, **48**, 489 (1972).
9) O. Haida, H. Suga, and S. Seki, *Proc. Japan Acad.*, **49**, 191 (1973).
10) O. L. I. Brown, W. V. Smith, and W. M. Latimer, *J. Amer. Chem. Soc.*, **58**, 1758 (1936).
11) R. Kiriyama, H. Ibamoto, and K. Matsuo, *Acta Crystallogr.*, **7**, 482 (1954).
12) K. Okada, M. I. Kay, D. T. Cromer, and I. Almodovar, *J. Chem. Phys.*, **44**, 1648 (1966).
13) K. C. Turberfield, *Solid State Commun.*, **5**, 887 (1967).
14) M. I. Kay and R. Kleinberg, *Ferroelectrics*, **4**, 147 (1972).
15) T. Matsuo, M. Oguni, H. Suga, and S. Seki, *Proc. Japan Acad.*, **49**, 196 (1973).
16) R. Kiriyama, H. Kiriyama, T. Wada, N. Niizeki, and H. Hirabayashi, *J. Phys. Soc. Japan*, **19**, 540 (1964).
17) J. C. Taylor, M. H. Mueller, and R. H. Hitterman, *Acta Crystallogr.*, **A26**, 559 (1970).
18) e.g., R. J. Birgeneau, H. J. Guggenheim, and G. Shirane, *Phys. Rev. Lett.*, **22**, 720 (1969); R. J. Birgeneau, J. Skalyo, and G. Shirane, *Phys. Rev.*, **B3**, 1736 (1971).
19) P. W. Kasteleijn, *J. Math. Phys.*, **4**, 287 (1963).
20) A review of this method is given by E. W. Montroll, in "Applied Combinatorial Mathematics," ed. by E. F. Beckenbach, Wiley, New York (1964), Chap. 4.
21) L. Onsager, *Phys. Rev.*, **65**, 117 (1944). See especially equation (7.5) in the Appendix.